

Supplementary Information

Dynamic Control of 3D Chemical Profiles with a Single 2D Microfluidic Platform

YongTae Kim, Sagar D. Joshi, Lance A. Davidson, Philip R. LeDuc*, and William C. Messner*

Supplementary Figures

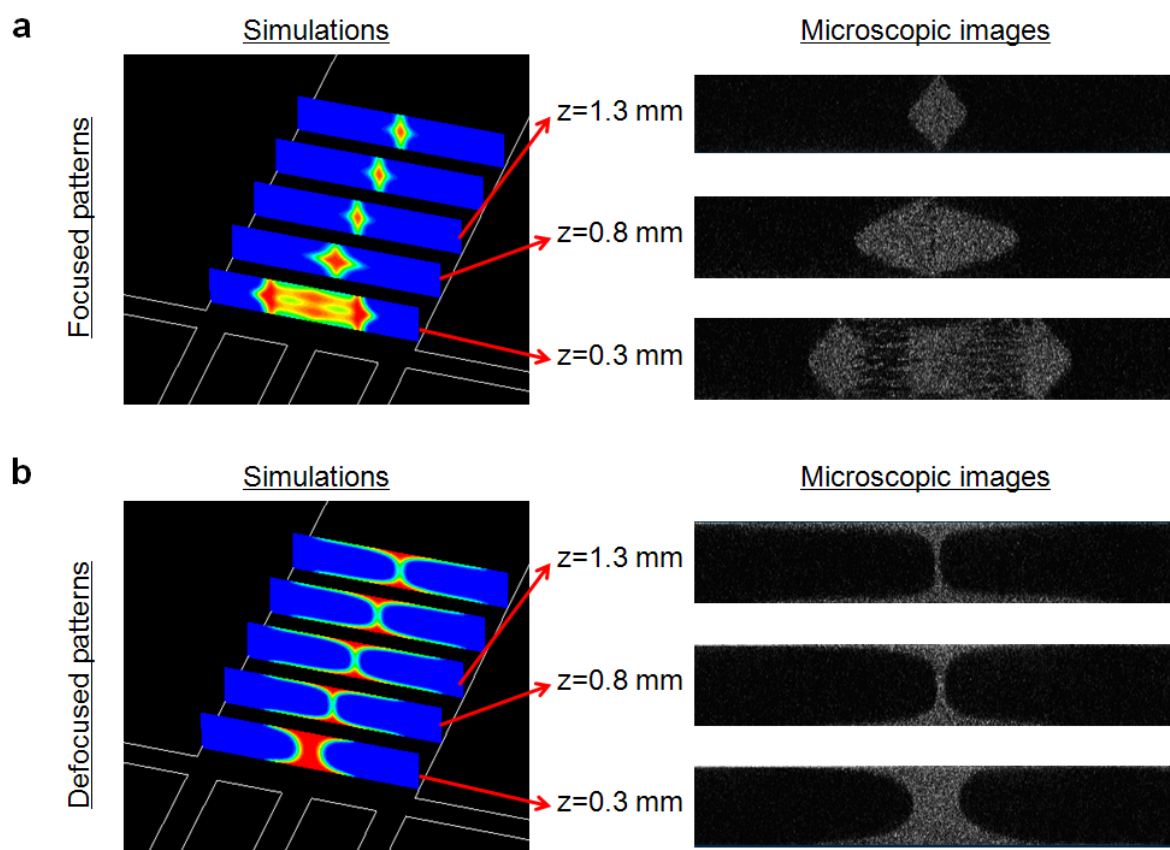


Fig. S1 Simulations and microscopic images of focused and defocused patterns in different locations (z -axis). **a)** Simulations of focused patterns at the sections at $z = 0.3, 0.8, 1.3, 1.8,$ and 2.3 mm and fluorescent images of focused patterns at the sections at $z = 0.3, 0.8,$ and 1.3 mm. **b)** Simulations of defocused patterns at the sections at $z = 0.3, 0.8, 1.3, 1.8,$ and 2.3 mm and fluorescent images of defocused patterns at the sections at $z = 0.3, 0.8,$ and 1.3 mm.

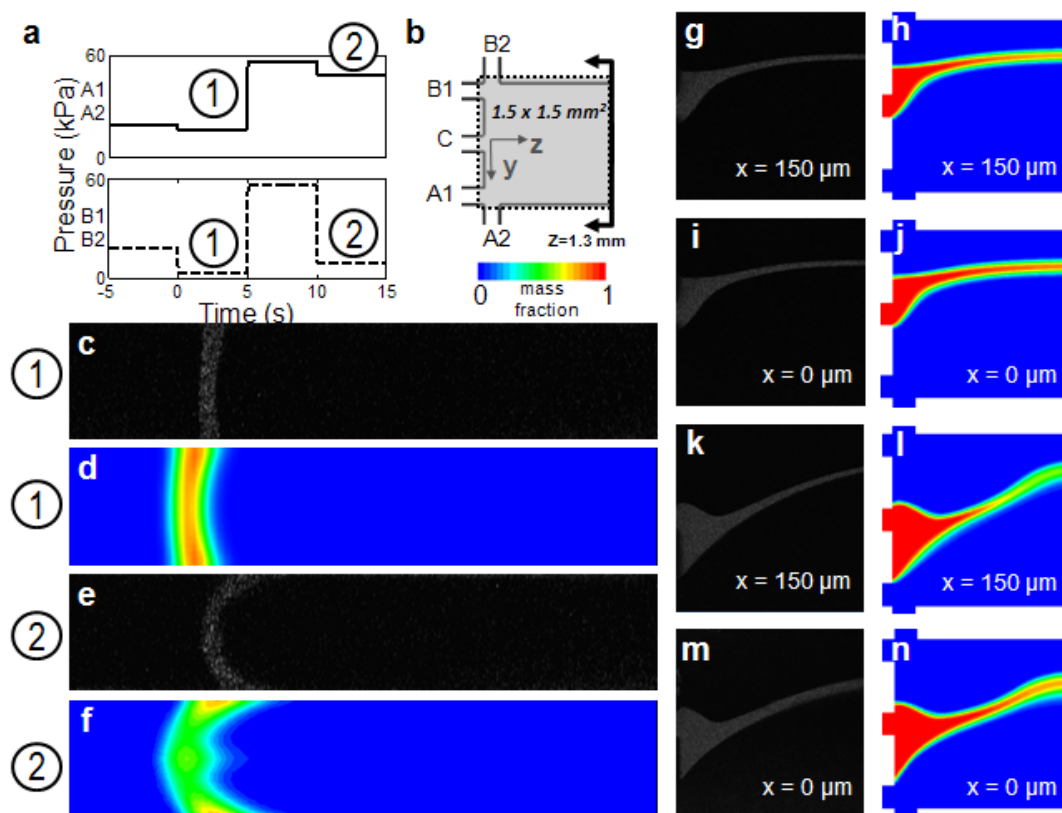


Fig. S2 Controlling the 3D patterns in the y direction. **a)** Pressure profiles over time. Each panel represents the inlet pressure level of the $+y$ side (A1 and A2) and the $-y$ side (B1 and B2) inlets, respectively. The pressure source was set at the same pressure of 28.5 kPa for 5 seconds, and the inlet pressures were precisely controlled in the pressure state ① (A1, A2: 16.0 kPa, B1, B2: 3.2 kPa) to move the central stream in the $-y$ direction at Reynolds number (~ 10). Then, the pressure source was increased to 56.4 kPa for 5 seconds from 5 to 10 seconds, and the inlet pressures were regulated in the pressure state ② (A1, A2: 48.0 kPa, B1, B2: 9.5 kPa) to move the central stream to the $-y$ direction at three times higher Reynolds number (~ 30). **b)** Coordinate system and range of imaging in the microfluidic channel. **c-f)** Fluorescent images and simulations at the section at $z=1.3$ mm for the pressure states ① and ② in a). **g-j)** Fluorescent images and simulations at the sections $x=150$ μm and $x=0$ μm for the case ① in a). **k-n)** Fluorescent images and simulations at the sections $x=150$ μm and $x=0$ μm for the case ② in a).

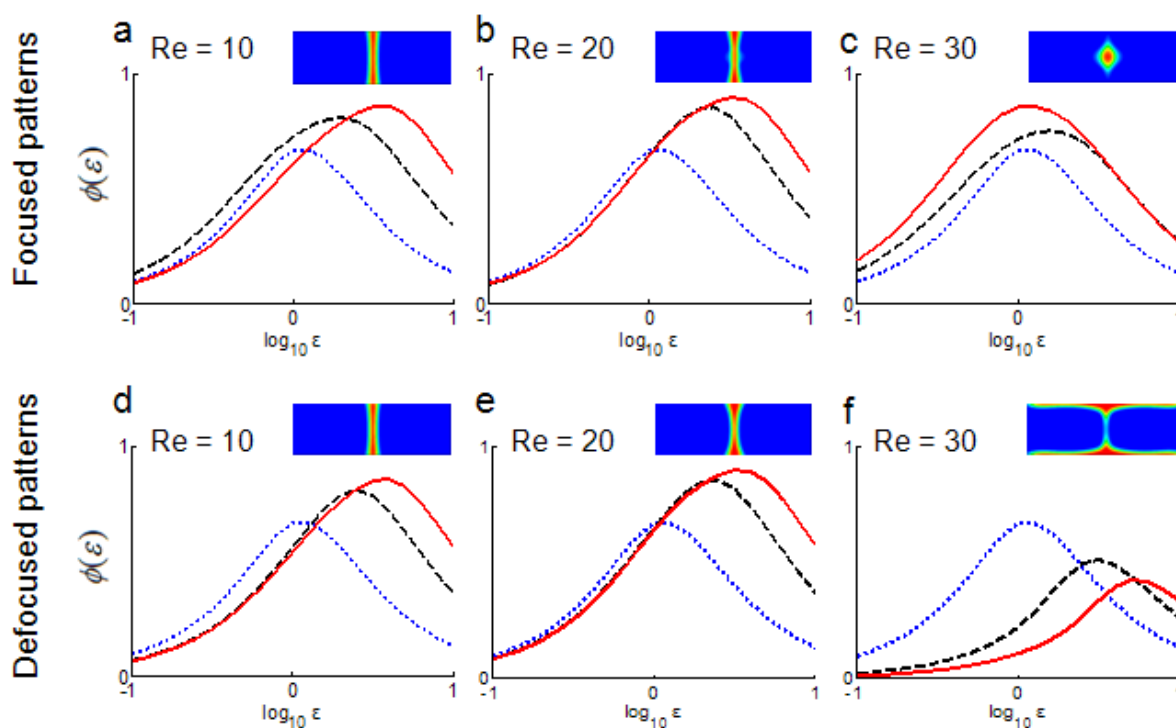


Fig. S3 Focus index Φ indicating the focused degree using the 2D Gaussian function for focused patterns at Reynolds number. **a)** 10, **b)** 20, and **c)** 30 and for defocused patterns at Reynolds number **d)** 10, **e)** 20, and **f)** 30. The dotted, dashed, and solid lines represent the focus index for channels with heights of 100, 300, and 500 μm , respectively. The inset section images for the channel height of 500 μm are from the table in Figure 4a and correspond to the solid line in each panel.

Supplementary Movies

Movie S1. Simulation depicting the 3D pattern transformation in the xy planes ($z = 1.3 \text{ mm}$) and yz ($x = 150 \text{ }\mu\text{m}$).

Movie S2. Confocal Microscopic 3D images showing the 3D patterns remained at a central location in the y direction at the middle of the channel ($x = 150 \text{ }\mu\text{m}$) and a location at the bottom of the channel ($x = 0 \text{ }\mu\text{m}$) (see Supporting Figure 1c-f).

Movie S3. Confocal Microscopic 3D images showing the patterns remained focused at a central location for the y-direction at the middle of the channel, but dispersed across the x-direction at the bottom of the channel (see Supporting Figure 1g-j).

Movie S4. Confocal Microscopic 3D images showing two microvortices inside the central stream (see Supporting Figure 1k-n).

Movie S5. Confocal Microscopic 3D images showing two microvortices outside the central stream (see Supporting Figure 1o-r).